Computational Modeling of Surface Energy and Structural Behavior of $Li_4P_2S_6$ Electrolytic Solid Interfacing with Lithium Anodes

A paper presented to the faculty of the Department of Physics of Wake Forest University in partial fulfillment of the requirements for graduation with Honors in Physics.

Cameron M. Kates

9th May, 2014

Approved by:

Dr. Natalie Holzwarth

Dr. Timo Thonhauser

Dr. David Carroll

Table Of Contents

I. Introduction

The study of lithium ion solid-state batteries is of continuing scientific importance due to their superior operational characteristics including, but not limited to, increased efficiency and stability when compared with older battery designs. As a result of their desirable traits, Li-ion batteries are experiencing widespread utilization in mobile devices, and other micro-battery and high energy demand applications. This growing interest and application of Li-ion batteries is the most general motivation for this project. Specifically, lithium thiophosphate solids have shown growing promise as electrolytic materials for use in these applications.[1] However, there are still many possible materials which have not been fully explored in this light. To that purpose, the goal of this project is to further examine the electronic and physical properties of one such thiophosphate material, $Li_4P_2S_6$ through computational modeling of the structure.

We have and are continuing to analyze the surface energy of both XY and YZ planar cleaves of the crystal, as well as the physical behavior and stability of the different crystal cleaves when placed in interface with lithium anodes. We then use these characteristics as qualifiers to establish the feasibility of $Li_4P_2S_6$ as an electrolytic material in Li-ion battery applications. We have chosen $Li_4P_2S_6$ in particular due to previous experimental projects which suggest that this material may be stable and favorable for our purposes. Initially, chemically similar thiophosphates were synthesized at Oak Ridge National Laboratory, after oxynitride based materials proved to be prohibitively non-conductive. These compounds showed promising stability as electrolytes. Additionally, Zachary Hood, who at the time was working in the Wake Forest University Chemistry Department, experimented with the synthesizing of $Li_4P_2S_6$ while working on various LiPON projects. Notes from his project show that the attempted synthesis of other similar materials results in the creation of $Li_4P_2S_6$, suggesting some inherent stability. Additionally, when left exposed to the atmosphere, synthesized $Li_4P_2S_6$ remained stable and did not degrade for some time. This too suggests that our material is stable enough to warrant further examination as a possible electrolytic material.

Additionally, $Li_4P_2S_6$ as we have modeled it possesses some other interesting characteristics when compared to other similar materials that have been both computationally and experimentally examined. Primarily, $Li_4P_2S_6$ has an extra phosphorous-phosphorous bond not present in materials like Li_3PS_4, which was computationally analyzed in a study published in the Physical Review by N.D. Lepley, N.A.W. Holzwarth, and Yaojun A. Du.[2] This additional phosphorous-phosphorous bond is formed as a result of the material's tendency to favor the more stable fully occupied shell, and it suggests that $Li_4P_2S_6$ is likely to exhibit some new and different binding properties of interest.

II. Methods

The $Li_4P_2S_6$ solid was modeled in this project using first principles computational methods utilizing Density Functional Theory. The primary software used was the public domain, open source PWscf code[3] from the Quantum Espresso suite. We also used XcrySDen[4] and VESTA[5] for visualizing the crystalline structures and their behavior.

A. Approximation Methods

PWscf, the principal code used in this project, functions by performing a series of approximations to accurately estimate the total energy of a given material. The "total energy," in this case, is the energy required to disassemble the material into separated ions and electrons, up to a systematic constant of the calculation. These energies are then used to determine the forces acting on each atom, and how those forces will affect their positions relative to the rest of the crystal (this process will be explained more thoroughly in part B of the Methods section). Of course, actually solving the exact many body Schrödinger equation problem to find the energies we desire is prohibitively time consuming (if nigh impossible), even computationally. Ultimately, PWscf relies mainly on the concepts of Density Functional Theory, or DFT, to determine this behavior.

So that we may justify our application of DFT, we must consider a number of approximations relating to the exact representation of the material. Before DFT can be applied, we must first view our atoms in a different light. Quantum mechanically, the electrons of an atom are much lighter than the nuclei, and as a result they are much more susceptible to the forces and interactions that we wish to approximate and model. We can exploit this to simplify our calculations using the Born Oppenheimer approximation, in which we treat the nuclei and the electrons of our atoms independently of one another.[6] This allows us to treat the nuclei as stationary, while we perform our (now much simpler) approximations for the electron energies. These calculations are performed using DFT.

Density Functional Theory operates on the principle that the ground state energy of the complicated many-electron Schrödinger equation can be represented using a unique functional of the electron density.[6] The functional refers to the mathematical functional, which maps a separate function (which is itself dependent on a series of variables, and which maps those variables to a unique answer) to another unique value. To this effect, we can represent the solution for the ground state energy of our many-body Schrödinger equation as the functional of the electron density as a function of position r, $\rho(r)$, and the ion positions, R_i, as shown in Equation 1 below.

Equation 1: Ground state energy as a functional of electron density and ion position.

$$E = f(\rho(r), R_i)$$

In *Equation 1*, the electron density can be defined in terms of all of the individual electron wave functions summed together, as shown by Sholl & Steckel in "Density Functional Theory," and in *Equation 2* below, where n_i is the occupation number.

Equation 2: ρ *as a function of individual electron wave functions* $\psi_i(r)$.[6]

$$\rho(\boldsymbol{r}) = \sum_{i(occ.)} n_i \psi_i^*(\boldsymbol{r}) \psi_i(\boldsymbol{r})$$

Finding the electron density which minimizes the energy equation shown in *Equation 1* will provide us with an accurate representation of the electron density which corresponds to the complete solution to the Schrödinger equation within density functional theory.[6] In other words, the Hamiltonian is the functional derivative of the electron density, ρ, as shown in *Equation 3* below.

Equation 3: H as the functional derivative of ρ.

$$-\frac{\delta(E)}{\delta(\rho(r))} = H$$

Now, we rewrite Schrödinger's equation as follows (*Equation 4):*

Equation 4:

$$H = -\frac{\hbar^2}{2m}\nabla^2 + \sum_{R_i} V_N(r - R_i) + V_H(\rho(\vec{r})) + V_{XC}(\rho(\vec{r}))$$

where V_N is the ionic potential, V_H is the Hartree potential, and V_{XC} is the exchange correlation potential. Note both the Hartree potential and the exchange correlation potential are dependent on the electron density, ρ(r). However, we can represent this as the Kohn – Sham equation, which expresses *Equation 3* in such a way that each potential relates to only one electron, rather than many, as shown in *Equation 5* below, where ψ is again the wave function for the individual electron, as it was in *Equation 2* above.[6]

Equation 5: Kohn-Sham Equations.

$$[-\frac{\hbar^2}{2m}\nabla^2 + V_N(r) + V_H(r) + V_{XC}(r)]\psi_i(\boldsymbol{r}) = \epsilon_i \psi_i(\boldsymbol{r})$$

Here, the Hartree potential represents the electron-electron interactions, and is defined by Sholl and Steckel as is shown in *Equation 6* below.

Equation 6: The Hartree Potential.[6]

$$V_H(\boldsymbol{r}) = e^2 \int \frac{\rho(\boldsymbol{r'})}{|\boldsymbol{r}-\boldsymbol{r'}|} d^3r'$$

That is, it represents repulsion between the electron in question and all of the other electrons in the structure (which are represented by the electron density ρ) due to Coulomb's law. Note here that there is an element of self-consistency introduced into the calculation: we are solving *Equation 5* so that we may find the wave function for the individual electron, and we need the Hartree potential to do so. However, both the Hartree potential and the exchange correlation potential are determined by the electron density, which we have in terms of the same wave functions for the single electron. This self-consistency is processed numerically within the functioning of the code. The PWscf software (and any regular DFT solution, for that matter) begins with a trial electron density function ρ_t, much like one would when using the variational principle. Then, the entire process, including solving the Kohn-Sham equation, is completed using this trial density to find a single particle wave function ψ_i based on the trial electron density ρ_t. Now that we have this single particle wave function ψ_i, we can use it to calculate a *new* electron density, ρ_n using *Equation 2* from above. This series of calculations is performed many times over, with the goal being the convergence of the new electron density ρ_n with the original test density, ρ_t. When the two densities converge nicely, they should both represent the correct ground state energy for the system.

In addition to the ionic potential and Hartree potential, there is also the exchange correlation potential, V_{XC}, "which defines exchange and correlation contributions to the single-electron equations," and is shown in *Equation 7* below.[6]

Equation 7: The Exchange Correlation Potential Functional.[6]

$$V_{XC}(r) = V_{XC}^{electrongas}[\rho(\boldsymbol{r})]$$

Note that the exchange correlation potential is achieved by approximating the potential using the known potential of the free electron gas and the electron density. In this case, ρ(r) is the local electron density at the location with which we are concerned. Thus the title "Local Density Approximation," or LDA functional.[7] The LDA functional was used for this project as it has a history of working well for the purposes of modeling non-transition metal insulating materials, much like our $Li_4P_2S_6$ crystal.

B. Functionality of PWscf

As explained in Part A of the Methods explanation above, the main software used in this project is PWscf, of the Quantum Espresso suite. The PWscf, or Plane-Wave Self-Consistent Field, package is capable of performing many different "calculations of electronic-structure properties within Density-Functional Theory (DFT), using a Plane-Wave (PW) basis set and pseudopotentials (PP)."[8] For this project, we are utilizing the PAW, or Projector Augmented Wave pseudopotential[9] datasets. The datasets used contain information regarding the pseudopotential, the all electron basis function, and the projector wave function that can be recognized by the software. These datasets were created in collaboration with Jamie Drewery, Zach Pipkorn, and Dr. Natalie Holzwarth as part of a project beginning in the Spring of 2013. Further information can be accessed at that project's web page.[10]

For our purposes, PWscf's ability to analyze and model ground state energies and single electron wave functions, leading to calculations of the atomic forces within the simulation cell is of the most use. Essentially, PWscf uses the principles of DFT discussed in part A above to find the energy of individual atoms or ions. From this, it is able to determine the force on each ion, using calculations based on *Equation 8* below.

Equation 8: Force on the ion, using atomic energy E.

$$-\frac{\partial E}{\partial \vec{R}_i} = \vec{F}_i$$

That is, the force on the ion is equal to the partial derivative of its energy with respect to it's current position. Once the force on each atom is known, PWscf can determine where each atom will move during the current cycle of the program. During the next cycle, the new position of the atom will be used to compute the energy, and in turn the new force. This progression will continue until the energy levels are sufficiently converged, and the final atomic positions are achieved.

C. Software Usage

For this project, PWscf is used in three main ways: modeling the behavior of the $Li_4P_2S_6$ crystal in a vacuum, calculating the surface energy of those crystals in the vacuum, and modeling the crystal in interface with lithium anodes, represented as layers of Li atoms placed a set distance away from the surface cleave which we intend to analyze.

1. Cleaving and Modeling of $Li_4P_2S_6$ in Vacuum

The first step in our modeling process was to define the notion of a "cleave" or a "layer" of our crystal. Our goal in cleaving the crystal is to expose an ideal surface of our crystal. To do this, we began with the original lattice supercell for $Li_4P_2S_6$, shown in *Figure 1* below.

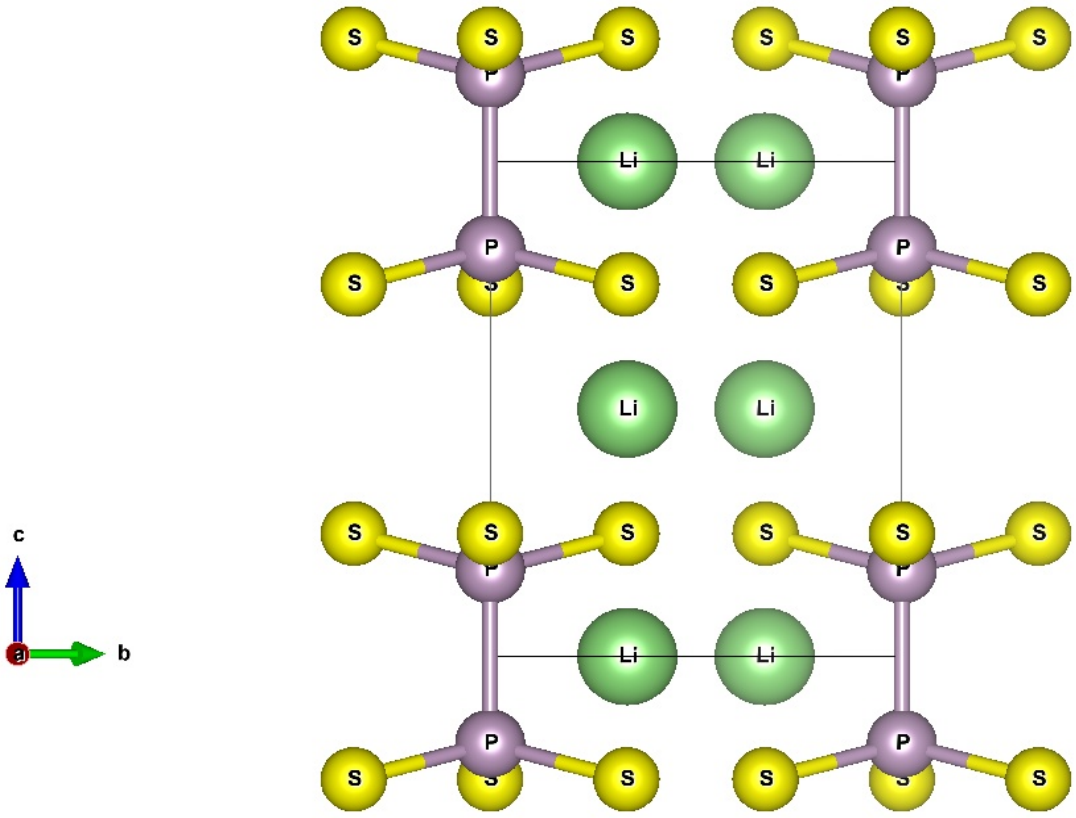

Figure 1: $Li_4P_2S_6$ Original Lattice.

In *Figure 1* we can see not only the expected sulfur – phosphorous bonds, but the extra phosphorous-phosphorous bonds at each corner of the unit cell which make $Li_4P_2S_6$ unique. If we rotate the crystal slightly and increase our coordinate boundaries so that more periodic repetitions of the crystal cells are displayed, we are able to see the hexagonal structure of the material, as shown in *Figure 2* below. Also included in *Figure 2* is a directional representation of our most common crystal cleaves, the XY and YZ planes.

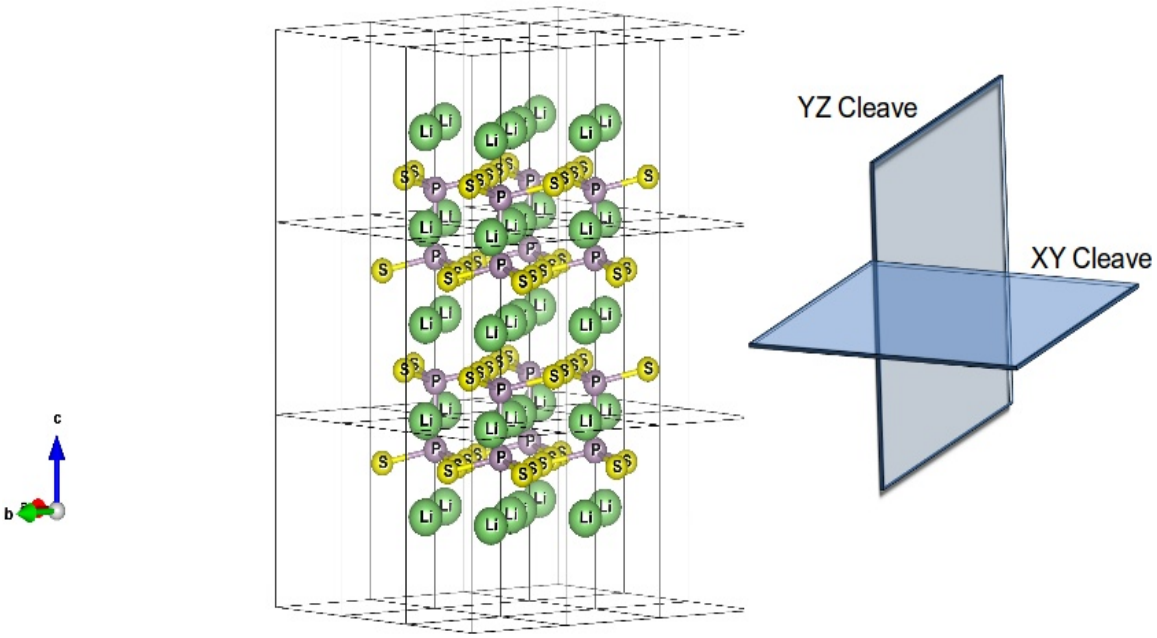

Figure 2: Original $Li_4P_2S_6$ supercell, with planar cleaves displayed.

When we cleave a crystal, we essentially cut it along a particular plane, leaving that plane of the crystal exposed. We are then able to perform surface energy calculations for the exposed surfaces, as well as test their stability in interface with lithium. This is useful, as it helps us to determine if a particular surface or configuration within the crystal is significantly more stable and desirable than another.

Typically, these cleaves are performed along predefined positions of the crystal, so that the structure may be cleaved into repeating layers of the same uniform size and shape. For example, in *Figure 3* below, we see two layers of an XY plane cleave, with cleave lines marked to define each layer.

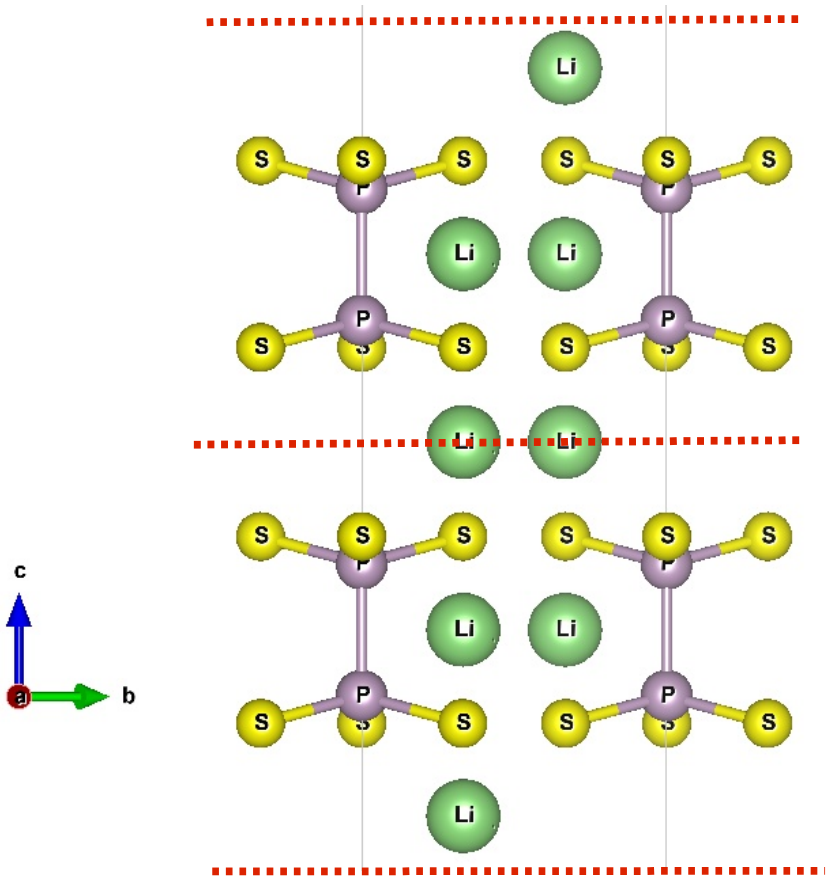

Figure 3: Two Layer XY Cleave.

Note how in this particular cleave, some of the lithium atoms are shared along the cleave boundary. Because of this, special care must be taken when determining the atomic positions for the cleaved crystal so that the asymmetrically placed Li atoms at the edge of the cleaves fit well with the next layer in the periodic repetition. As another example, a two layer YZ plane cleave is shown in *Figure 4* below, again with the cleave lines marked to define layers. Note that to ease the visualization of the YZ cleave the axes used are rotated from those of the original supercell. In *Figure 4* below, and in all plots of YZ cleaves, the primed axes should be taken to be as follows: **a'** = **a**, **b'** = **c, c'** = **-a**+2**b**. That is, **c'** is perpendicular to the other two primed vectors.

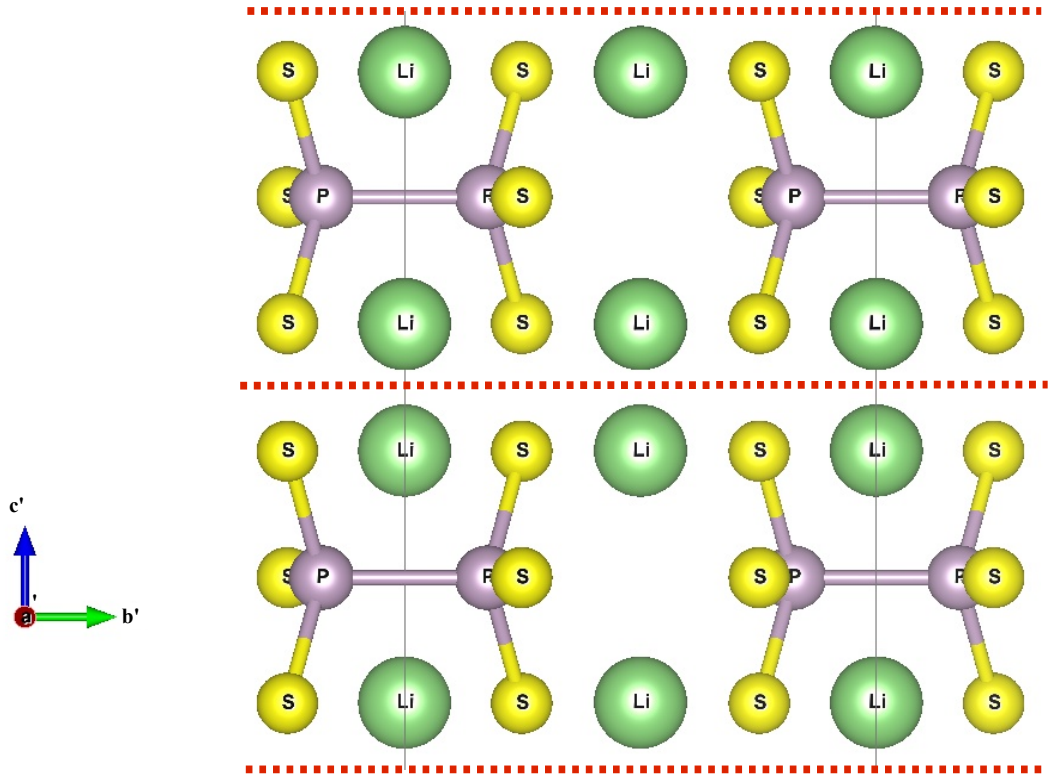

Figure 4: Two Layer YZ Cleave.

Achieving these cleaves is relatively straight forward, if not somewhat time consuming. To accurately complete this process, we utilized the XcrySDen visualization software. Although XcrySDen was used to visualize almost all of the structures pertaining to this project, it was especially useful when making modifications, like a cleave or layer addition, to the input file. XcrySDen allows the user to load a PWscf run file and examine the position of the atoms from the file before the run is actually submitted to the cluster, so we are able to fine tune the coordinates of each atom before committing CPU time to the computation. We begin with a crystal supercell structure which contains more layers than we would like, then utilize XcrySDen's ability to report the coordinates of each atom in the appropriate crystal-primitive coordinates to determine which atoms must be removed. Then, we can manually edit the list of atomic coordinates in the PWscf input file, removing those which we intend to cleave off. Once the crystal is cut down to the desired size and shape we are able to submit the run.

A PWscf run submitted to the cluster can be carried out in many different ways, depending on the input parameters specified in the run file. Besides the atomic positions themselves, our most used command parameter is the “calculation” input, which determines the structural optimization strategy for the run.

Typically, for models of the crystal in a vacuum like those shown in *Figure 3* and *Figure 4* above, we use “relax”:

```
:calculation = 'relax',
```

“Relax” specifies a fixed-cell type optimization, where the atoms are allowed to move as a result of the forces on them, but the unit cell containing them is fixed in dimension.

2. Calculating Surface Energies

Calculating the surface energies of the various cleave and layer combinations is of importance to our project, as lower, consistent energy levels suggest a higher degree of energetic stability for a particular crystal face. This is because a lower energy typically means the surface will be more likely to form in a vacuum. This does, however, assume that the system has reached equilibrium at a very low temperature (our calculations are performed at zero temperature). We calculated the surface energies of our crystal cleaves using the formula shown in *Equation 9* below, where E_{final} is the total energy of the crystal supercell after PWscf has run and the crystal has been allowed to relax; n is the number of formula units (or crystal cleave layers, in our case), E_{bulk} is the total energy per formula unit in the bulk structure (the perfect crystal), and A is the area of the surface.

Equation 9: Surface Energy Equation.

$$E_{final} = nE_{bulk} + A(E_{surface})$$

All of these values are included as part of the output file from PWscf. The values for E_{final} and n are known for the crystal surface of interest, and E_{bulk} is calculated using the original bulk structure calculations from the files of Dr. Natalie Holzwarth. These values are then simply compiled in a spreadsheet and $E_{surface}$ is calculated algebraically.

3. Adding Lithium Anode Interface Layers

In an actual physical battery system, the $Li_4P_2S_6$ crystal would be placed in close proximity with a lithium anode layer. We approximate this interface by inserting uniform layers of lithium atoms into our computational models of the crystal at some set small distance away. Carrying out this process again requires the use of XcrySDen's capabilities for determining atomic positions. Once the coordinates of the exposed crystal face have been located, new lithium atoms can be manually added to the list of atomic positions in the PWscf file. Typically, new lithium atoms are positioned about 5Å away from the crystal face. An example of a slab of $Li_4P_2S_6$ in interface with a lithium anode is pictured in *Figure 5* below.

Note that this is the two layer XY cleave from *Figure 3* with a uniform layer of lithium added below it.

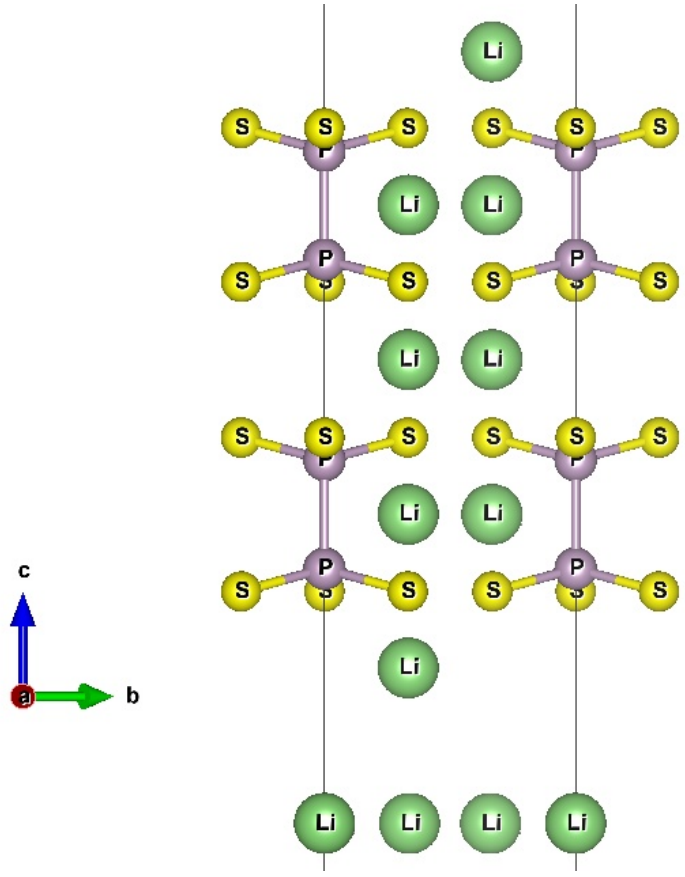

Figure 5: Two layer XY cleave in interface with single Li layer.

For lithium interface runs, we typically set the structural optimization method to allow variable cell relaxation, or "vc-relaxed":

```
:calculation = 'vc-relaxed',
```

"Vc-relaxed" does much of what its name suggests, and allows the unit cells which contain the crystal to expand and contract as the atoms move within them. However, one must also specify the coordinate direction in which we want to allow cell size variation. Our crystals are typically oriented in such a way that we wish for the atoms to move only in the **z** direction.

To assure this is the case, we add the input parameter “cell_dofree” (among other things) to the variable-cell optimization/dynamics portion of the input file (designated by &CELL):

```
:&CELL
:   cell_dofree = 'z'
```

We prefer to use vc-relaxed for lithium interface runs, as we are primarily concerned with the physical behavior of both the lithium atoms as well as the stability and behavior of the crystal structure itself. Permitting the unit cells to vary in this manner allows for more movement of the atoms, which helps us to better observe any instabilities in terms of atomic bonds being formed or broken due to the migration of the lithium atoms towards and through the $Li_4P_2S_6$ crystal.

III. Results

A. Surface Energy Calculations

Surface energy calculations for each cleave were completed using *Equation 9* and the process outlined in Part 2 of the Software Methods section of this document. Relevant results have been compiled in *Table 1*.

Table 1: Surface energy calculations.

XYSURFACE			
Layer	Efinal (Ry)	Esurface (Ry)	E_bulk: -548.2171 (Ry)
1	-548.1081	0.000496879	
2	-1096.3250	0.000498248	
3	-1644.5422	0.000497335	
4	-2192.7593	0.000498248	
YZSURFACE			
Layer	Efinal	Esurface	
1	-548.0588	0.000584574	
2	-1096.2805	0.000567956	
3	-1644.4998	0.000598317	
5	-2740.9318	0.000567587	
7	-3837.3663	0.000566479	

As can be seen in *Table 1* above, the XY surface cleaves typically exhibit lower surface energies, regardless of the number of layers present.

B. Physical Behavior of Crystal in Interface with Li Anodes

For this portion of the project, we chose to focus primarily on three, four, and five layer cleaves, as we felt that they provided a sufficiently large range of sizes while not becoming so large that they required prohibitively long amounts of computational time. In each case, figures for both pre and post-relaxation (pre-run submission and post-run submission) versions of the crystal are displayed. Additionally, plots of the structure's energy and volume over time are included.

1. Three Layer XY Cleave

Three XY cleave layers in interface with a double layer of lithium atoms, placed approximately 4.936 Å away from the cleaved XY surface.

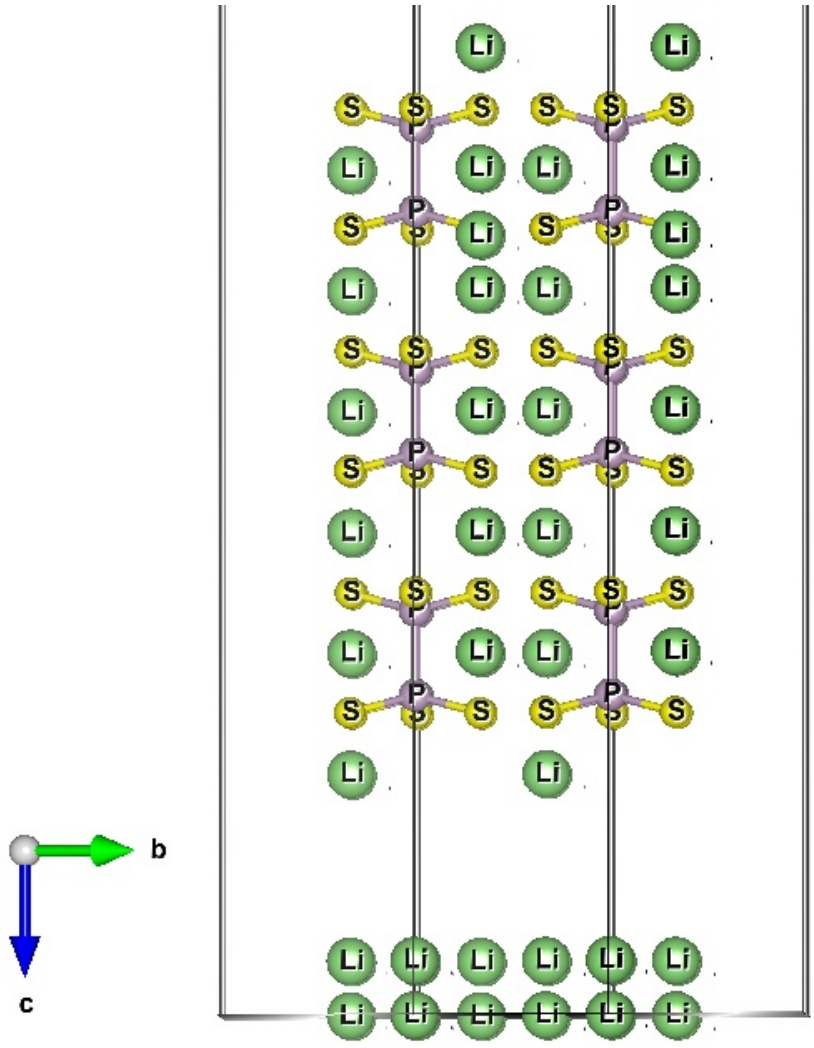

Figure 6: Three layer XY cleave in interface with double layer lithium anode, before relaxation.

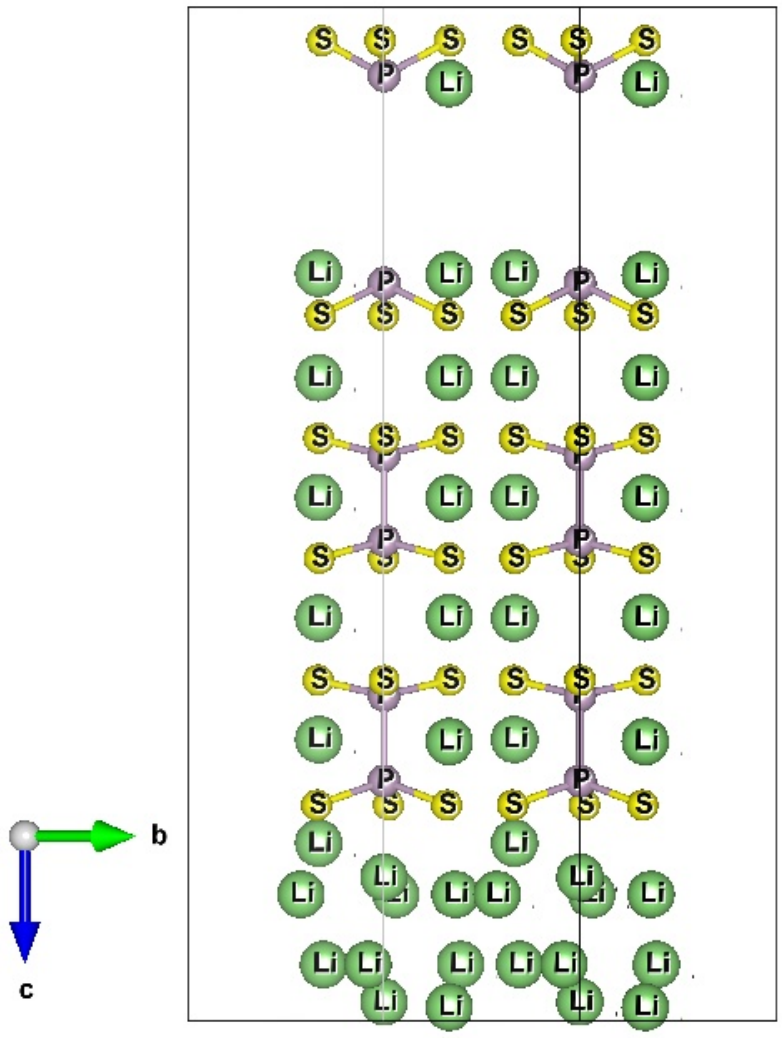

Figure 7: Three layer XY cleave in interface with double layer lithium anode, after relaxation.

The three layer XY cleave crystal exhibited interesting behavior when allowed to relax. The behavior at the bottom of *Figure 7* is relatively typical for an XY cleave, in that we see some migration of the lithium atoms towards the bottom of the crystal, but few to no atomic bonds being broken or formed within the $Li_4P_2S_6$ material itself. However, as can be seen in *Figure 7,* we observed the portion of the crystal furthest from the the lithium anodes breaking off and pushing away from the rest of the structure. The reasoning behind this behavior is not yet fully understood, but there are several hypothetical explanations. It is possible that some interesting chemical or electrical interactions are occurring within the crystal, causing the upper layer to experience a repulsive force, causing it to break away. Additionally, it is also possible that the top portion of the crystal

is not experiencing a repulsive force due to the lithium anodes below it, but an attractive force due to the lithium present in the periodic repetition above it. *Figure 8* is included below to show the proximity of the periodic cell repetitions in the **z** direction, and to illustrate how this may be possible. Atomic labels are not displayed in these plots for clarity, but atoms are color and size coded as in other plots.

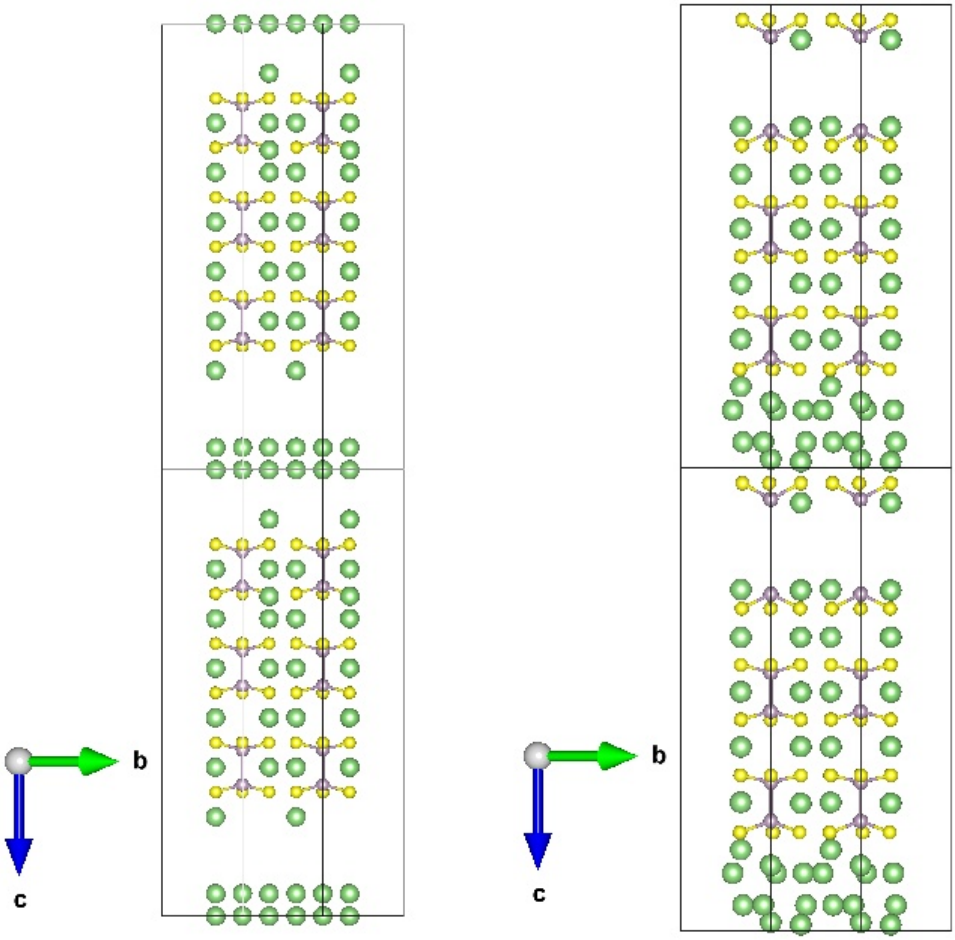

Figure 8: Periodic repetition of the 3 layer XY cleave in interface with Li before (left) and after (right) relaxation.

In *Figure 8* it is possible to see how the middle lithium layer seems to attract the top portion of the bottom crystal, then pull it upwards as the lithium migrates into the crystal above. Additionally, it is possible that this effect is actually non-physical, and is a side effect of the functioning of the visualization software. In either case, both plots of the energy and volume of this structure over time suggest good convergence. In the energy plot shown in *Figure 9* below, we see a sharp decrease in energy, then a steady line to the end of the run, showing a well converged energy value. In *Figure 10* below we see the volume contraction of the structure as it is allowed to relax over time.

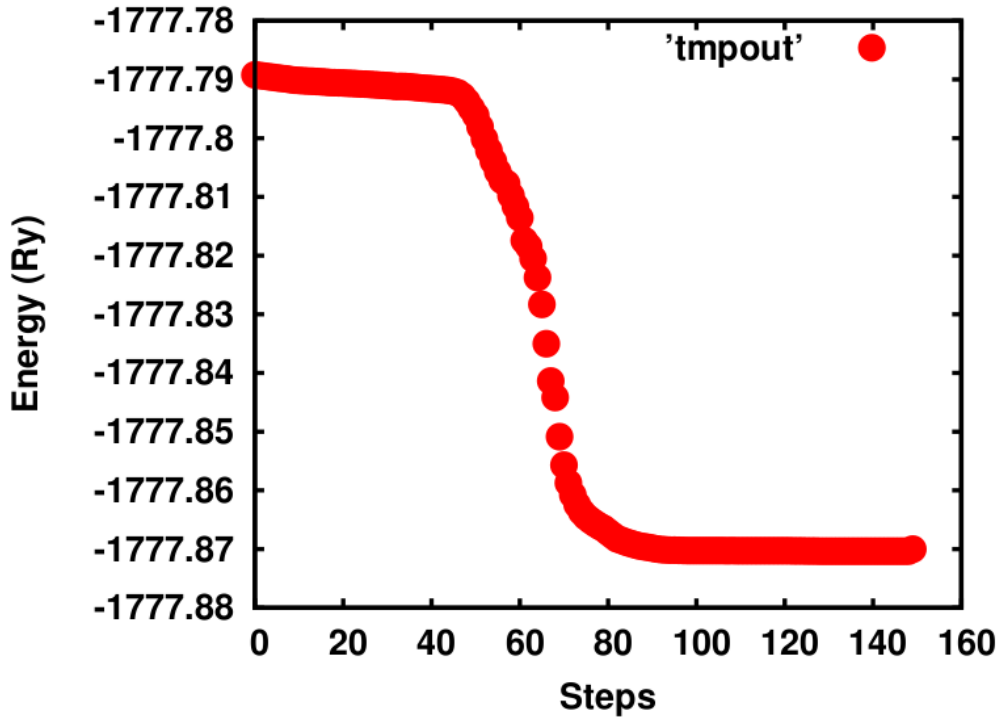

Figure 9: Changes in energy for 3 layer XY plane cleave in interface with double layer Li anode.

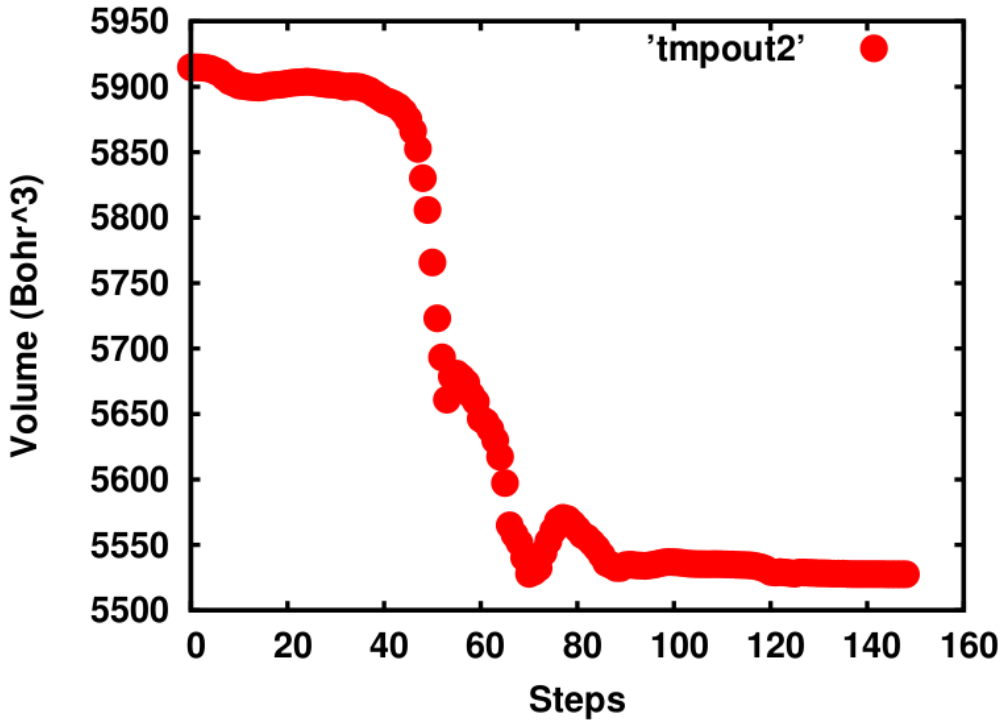

Figure 10: Volume contraction for 3 layer XY plane cleave in interface with double layer Li anode.

In *Figure 10*, we see the expected decline in volume as the lithium atoms migrate towards the crystal, reducing the overall volume of the system. However, after the minimum at around 85 steps in the plot we see a brief increase in the volume before it reaches equilibrium. It is possible that this indicates the moment at which the top portion of the crystal was removed from the main body of the crystal. Were that section of the crystal slowly pulled from the structure, it would cause an increase in the volume, as there would be some degree of stretch before the crystal was broken. This could result in the small increase and decrease in the volume. It is also possible that this represents a slight oscillation of the crystal's volume as it is compressed to its minimum, then rebounds out slightly before converging. Either way, more explanation of this situation is desired, and it is part of the ongoing focus of this project.

2. Four Layer XY Cleave

Four XY cleave layers in interface with a triple layer of lithium atoms, placed approximately 4.613 Å away from the cleaved XY surface. As was done for the three layer XY cleave above, the periodic repetition of the crystal in the modeling software is shown to better visualize the atoms residing near the cell boundaries. The four layer XY cleave is shown in interface with the triple layer lithium anode in Figure 11 below. Atomic labels are not displayed in these plots for clarity, but atoms are color and size coded as in other plots.

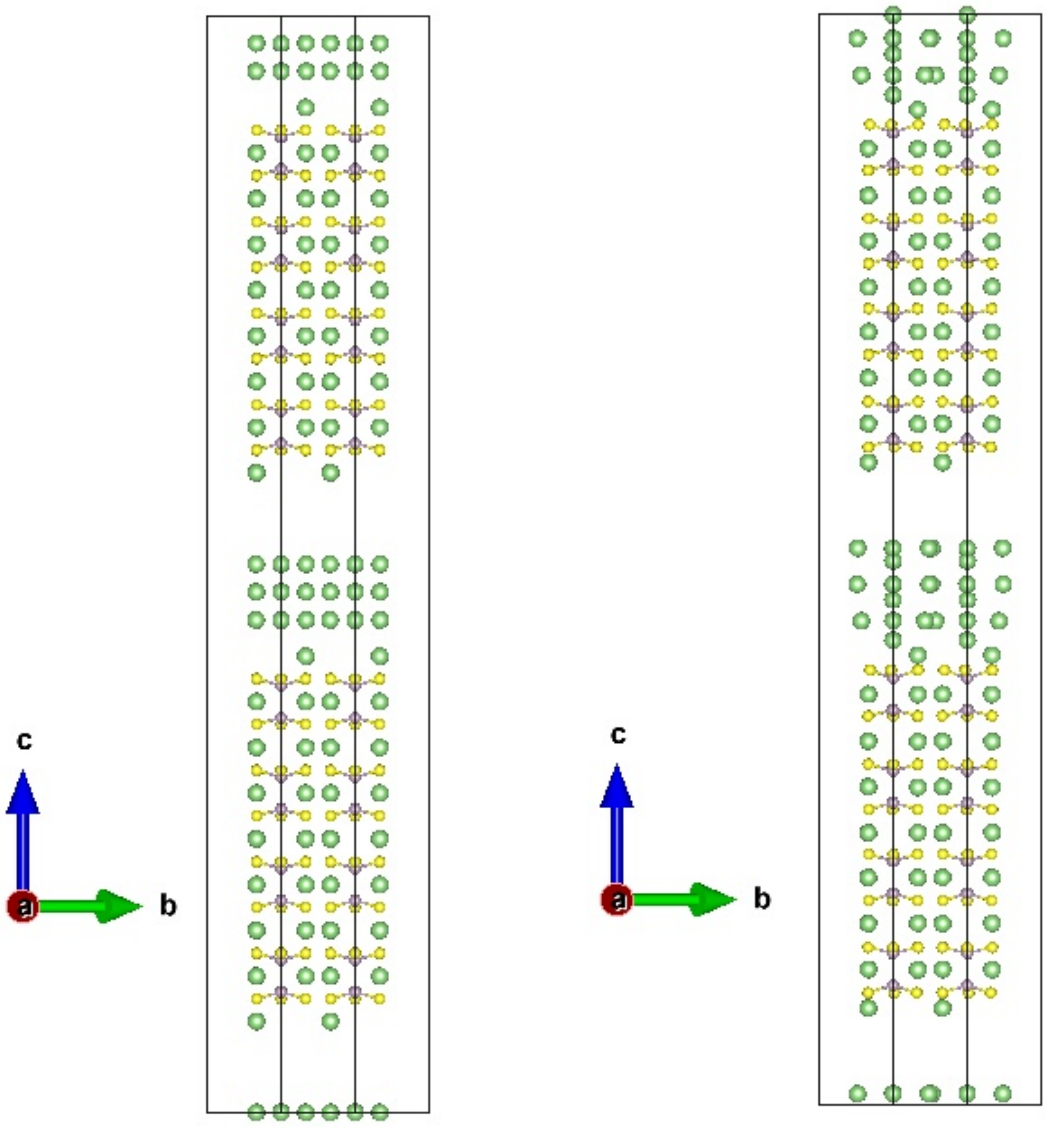

Figure 11: Periodic repetition of the 4 layer XY cleave in interface with Li before (left) and after (right) relaxation.

In *Figure 11* we again see that behavior of the crystal and lithium anodes in interface suggests some degree of stability present in the XY surface cleave. Note that there is some migration of the lithium atoms towards the surface of the crystal, but few to none moved into the crystal structure. Additionally, no phosphorous-phosphorous or sulfur-phosphorous bonds were broken, and no new bonds were formed.

Figure 12 (below) plots the energy for this structure over time, and again suggests good convergence, though this system is being allowed to relax again as of the writing of this document in an attempt to assure accuracy.

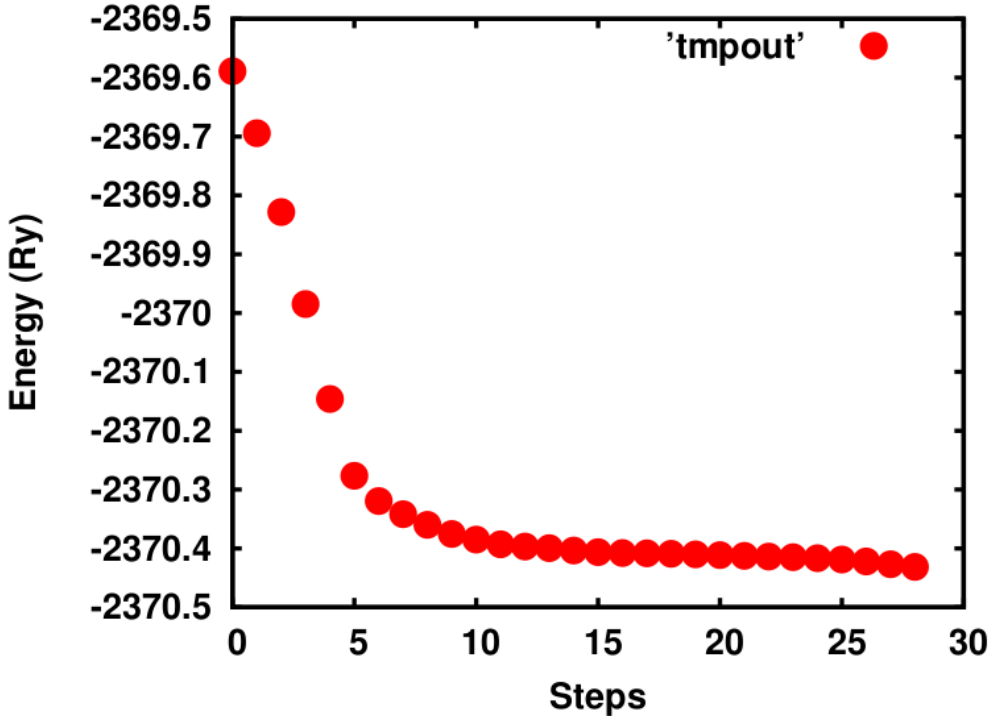

Figure 12: Changes in energy for 4 layer XY plane cleave in interface with triple layer Li anode.

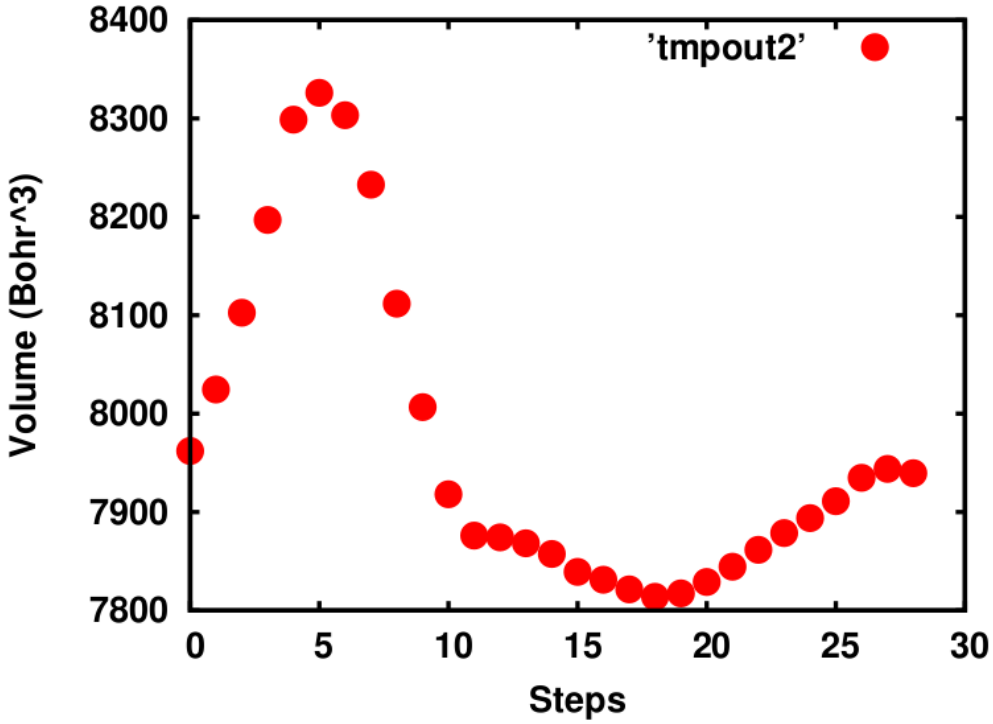

Figure 13: Volume contraction for 4 layer XY plane cleave in interface with triple layer Li anode.

Figure 13 (above), which represents the volume of the structure over time shows a downward trending fluctuation which also suggests that the system could use further relaxation before reaching complete convergence. Nonetheless, the steady energy values and stable behavior shown in the *Figure 11* visualization implies overall stability for this surface cleave and layer combination.

3. Three Layer YZ Cleave

Three YZ cleave layers in interface with a single layer of lithium atoms, placed 5.156 Å away from the cleaved YZ surface.

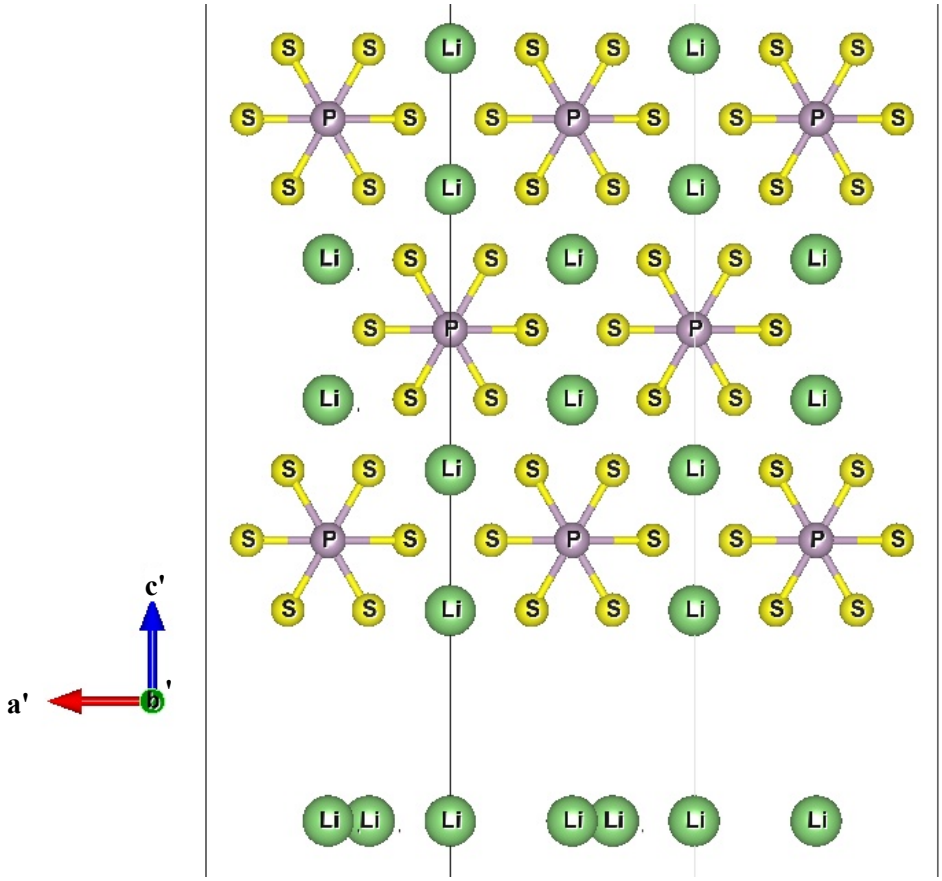

Figure 14: Three layer YZ cleave in interface with single layer lithium anode, before relaxation.

It should be noted that while the lithium atoms placed below the crystal may appear to be arranged in a non-uniform fashion, they are considered uniform for the purposes of our calculation. Due to the infinitely repeating periodic nature of the crystal models, the visualization software sometimes appears to add or delete atoms placed near the

boundaries of the unit cells. These effects are not, in fact, physical, and the calculations continue as intended.

.

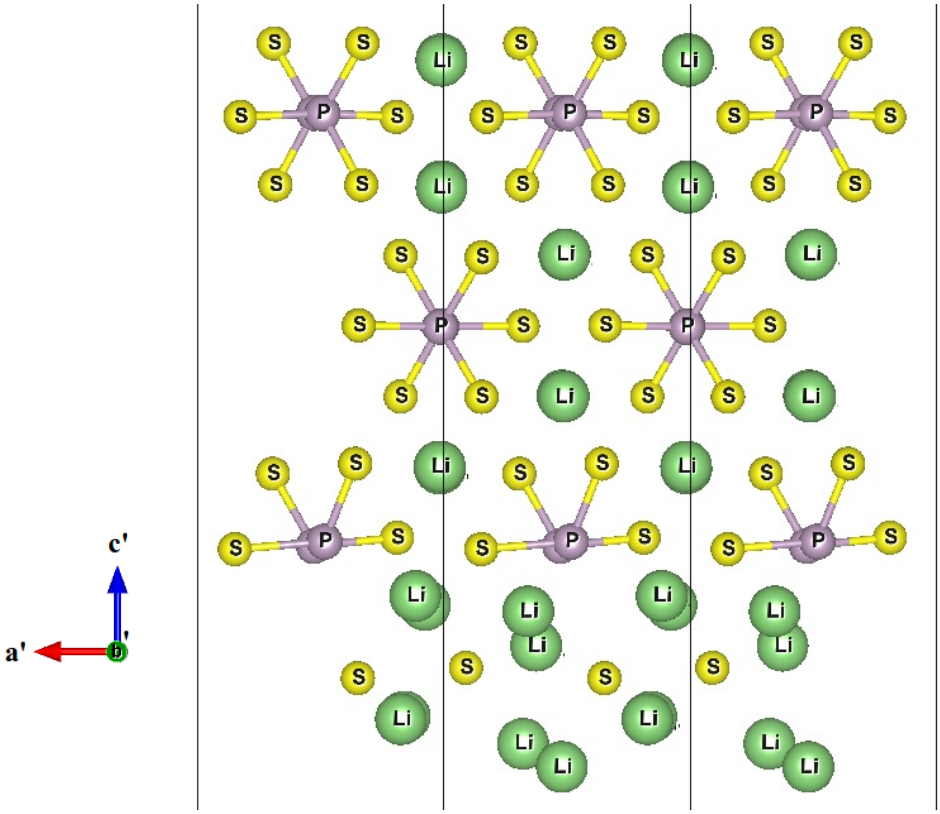

Figure 15: Three layer YZ cleave in interface with single layer lithium anode, after relaxation

When allowed to relax, the lithium atoms tended to migrate upwards into the $Li_4P_2S_6$ solid. As can be seen in *Figure 15* above, the migration of the lithium into the crystal resulted in the breaking of several sulfur-phosphorous and phosphorous-phosphorous bonds. Additionally, portions of the crystal structure were pulled from their original locations and removed from the scope of this particular visualization, as can be seen when comparing the lower left corners of *Figures 14* and *15*.

Figures 16 and *17* below show the changes in energy and volume contraction over time as this structure was allowed to relax.

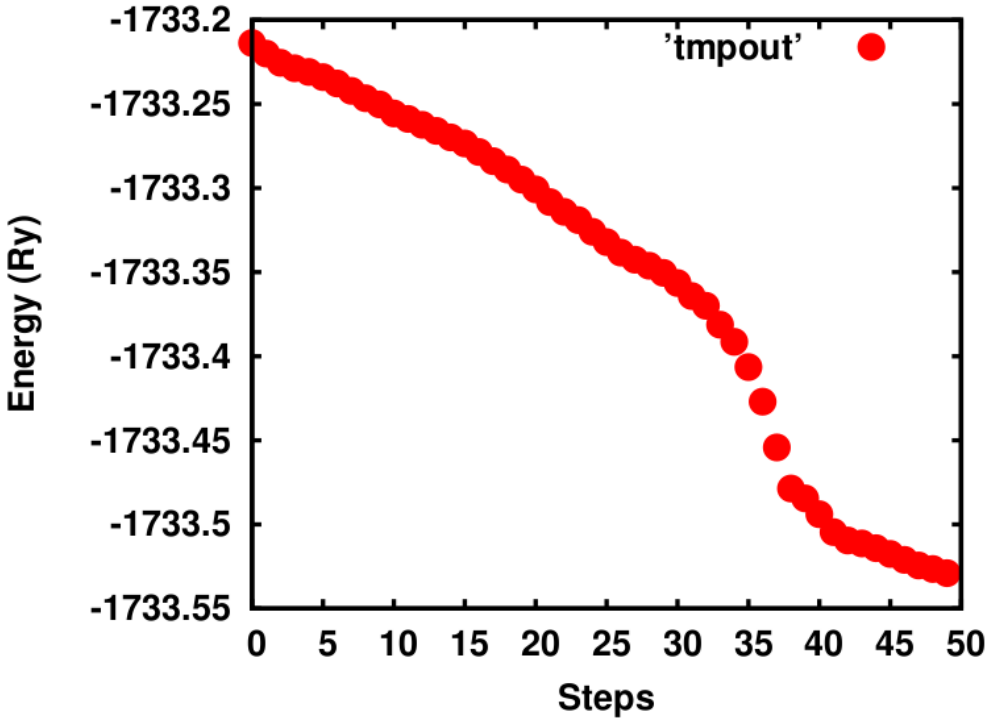

Figure 16: Changes in energy for 3 layer YZ plane cleave in interface with single layer Li anode.

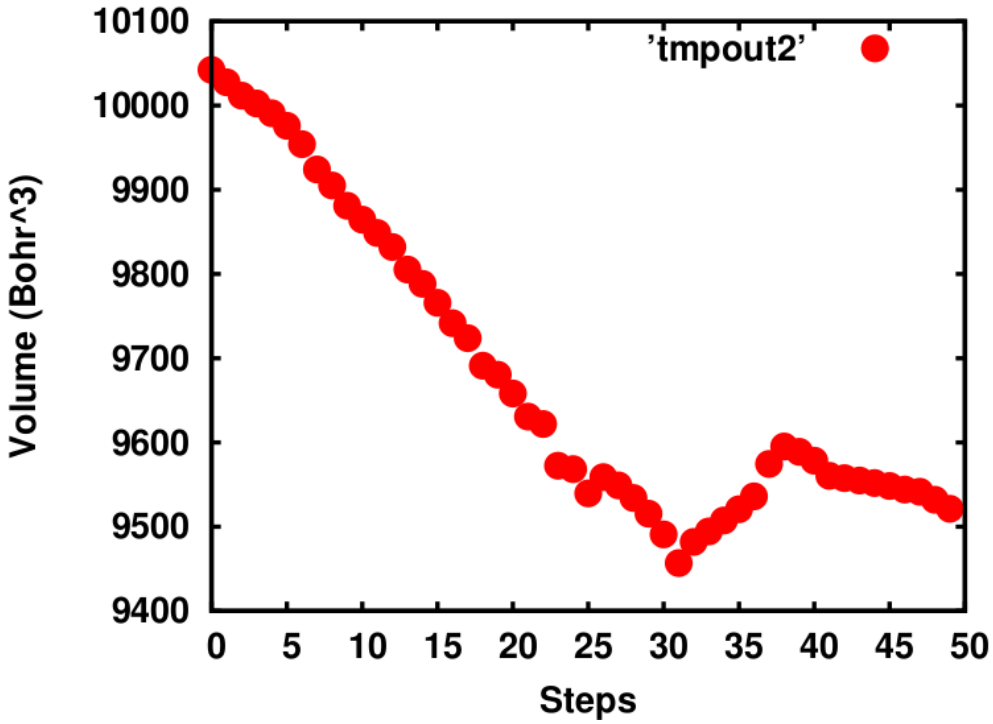

Figure 17: Volume contraction for 3 layer YZ plane cleave in interface with single layer Li anode.

In *Figure 16* we see a trend towards convergence in the energy, though the plot is in fact not as linear at later times as is seen in the XY energy plots above (*Figure 12* and *Figure 13*). Because of this, we are continuing to run files for this structure, allowing it to relax and the energy to converge further. Still, we feel that the results for this run are accurate.

C. Summary

At the time of the writing of this document, the XY planar cleaves of $Li_4P_2S_6$ show possible promise as the more stable cleave in physical battery systems. The XY cleaves tend to show lower surface energies, as shown in *Table 1*. Additionally, the XY cleaves typically experience less physical effects when placed in interface with the Lithium anode. Although this project is continuing, and it is not yet possible to be entirely certain of the viability of the $Li_4P_2S_6$ crystal XY plane as a electrolytic battery material, these factors do combine to suggest that further analysis of this material could be beneficial, as it does show some merit.

Currently, this project is ongoing, as we continue to run more test cases similar to those described in this document. Additionally, the structures examined up until this point are considered metastable, and we are interested in examining lower energy (if not ground state) versions of these materials using similar methods. There are also plans to possibly have this material synthesized and examined experimentally.

IV. Acknowledgements

The author would like to acknowledge support by NSF Grant DMR-1105485. All computations were performed on the Wake Forest University DEAC cluster, a centrally managed resource with support provided by the University. Additionally, the author would like to thank Dr. Natalie Holzwarth, Nicholas Lepley, Jamie Drewery, and Zachary Hood for their helpful advice.

V. References

1. Z. Liu, W. Fu, E. A. Payzant, X. Yu, Z. Wu, N. J. Dudney, J. Kiggans, K. Hong, A. J. Rondinone, and C. Liang, J. Am. Chem. Soc. **135**, 975 (2013).
2. N. A. W. Holzwarth, N. D. Lepley, and Y. A. Du, J. Power Sources **196**, 6870 (2011).
3. P. Giannozzi et al., J. Phys.: Condens. Matter **21**, 394402 (2009); available from the website http://www.quantum-espresso.org.
4. A. Kokalj, Journal of Molecular Graphics and Modeling **17**, 176 (1999), code available at the website http://www.xcrysden.org.
5. K. Momma and F. Izumi, Applied Crystallography **44**, 1272 (2011), code available from the website http://jp-minerals.org/vesta/en/.
6. D. S. Sholl, and J. A. Steckel, (2009), *Density Functional Theory – A Practical Introduction*, John Wiley & Sons, Hoboken, New Jersey, 238p.
7. J. P. Perdew and Y. Wang, Phys. Rev. B **45**, 13244 (1992).
8. P. Giannozzi, and M. Towler, *User's Guide for PWscf*, V. 5.0.2, DEMOCRITOS, pg. 2.
9. P. E. Blöchl, Phys. Rev. B **50**, 17953 (1994).
10. http://users.wfu.edu/natalie/papers/pwpaw/man.html.